ABSTRACT

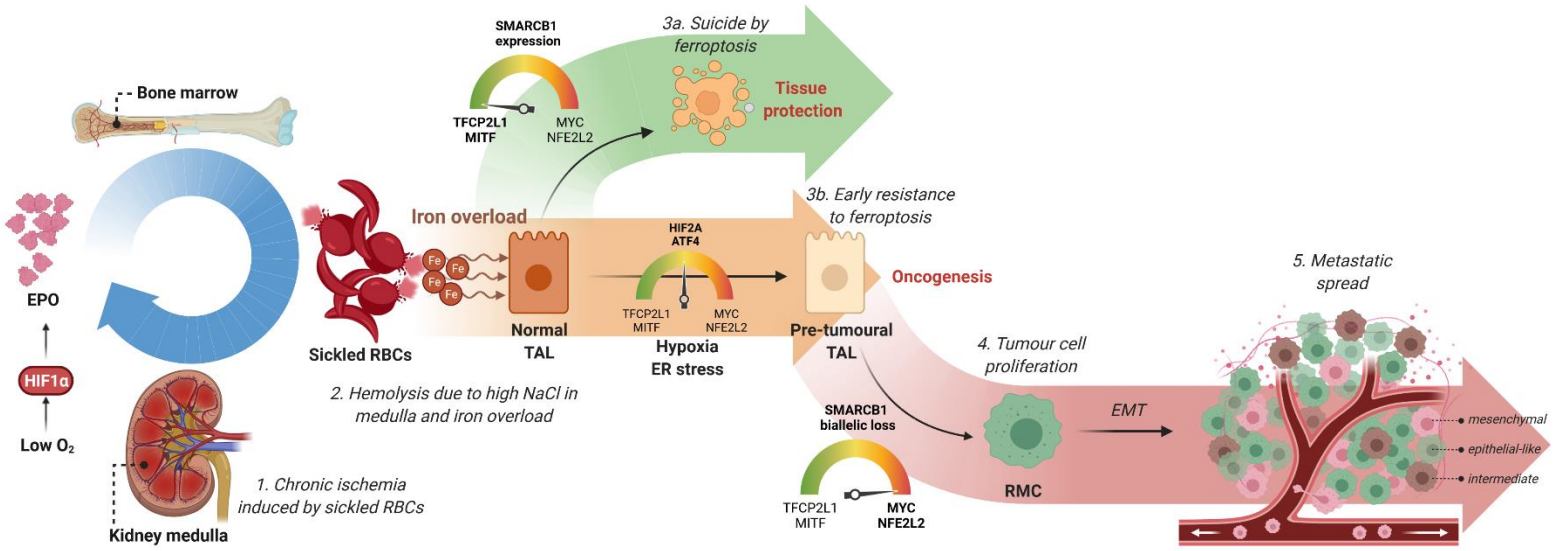

Renal medullary carcinoma (RMC) is an aggressive tumour driven by bi-allelic loss of SMARCB1 and tightly associated with sickle cell trait. However, the cell-of-origin and oncogenic mechanism remain poorly understood. Using single-cell sequencing of human RMC, we defined transformation of thick ascending limb (TAL) cells into three RMC cell states along an epithelial-mesenchymal gradient by loss of renal epithelial transcription factors TFCP2L1, HOXB9 and MITF and gain of MYC and NFE2L2-associated oncogenic and ferroptosis resistance programs. We describe the molecular basis for this transcriptional switch that is reversed by SMARCB1 re-expression repressing the oncogenic and ferroptosis resistance programs leading to ferroptotic cell death. Ferroptosis resistance links TAL cell survival with the high extracellular medullar iron concentrations associated with sickle cell trait, an environment propitious to the mutagenic events associated with RMC development. This unique environment may explain why RMC is the only SMARCB1-deficient tumour arising from epithelial cells, differentiating RMC from rhabdoid tumours arising from neural crest cells.

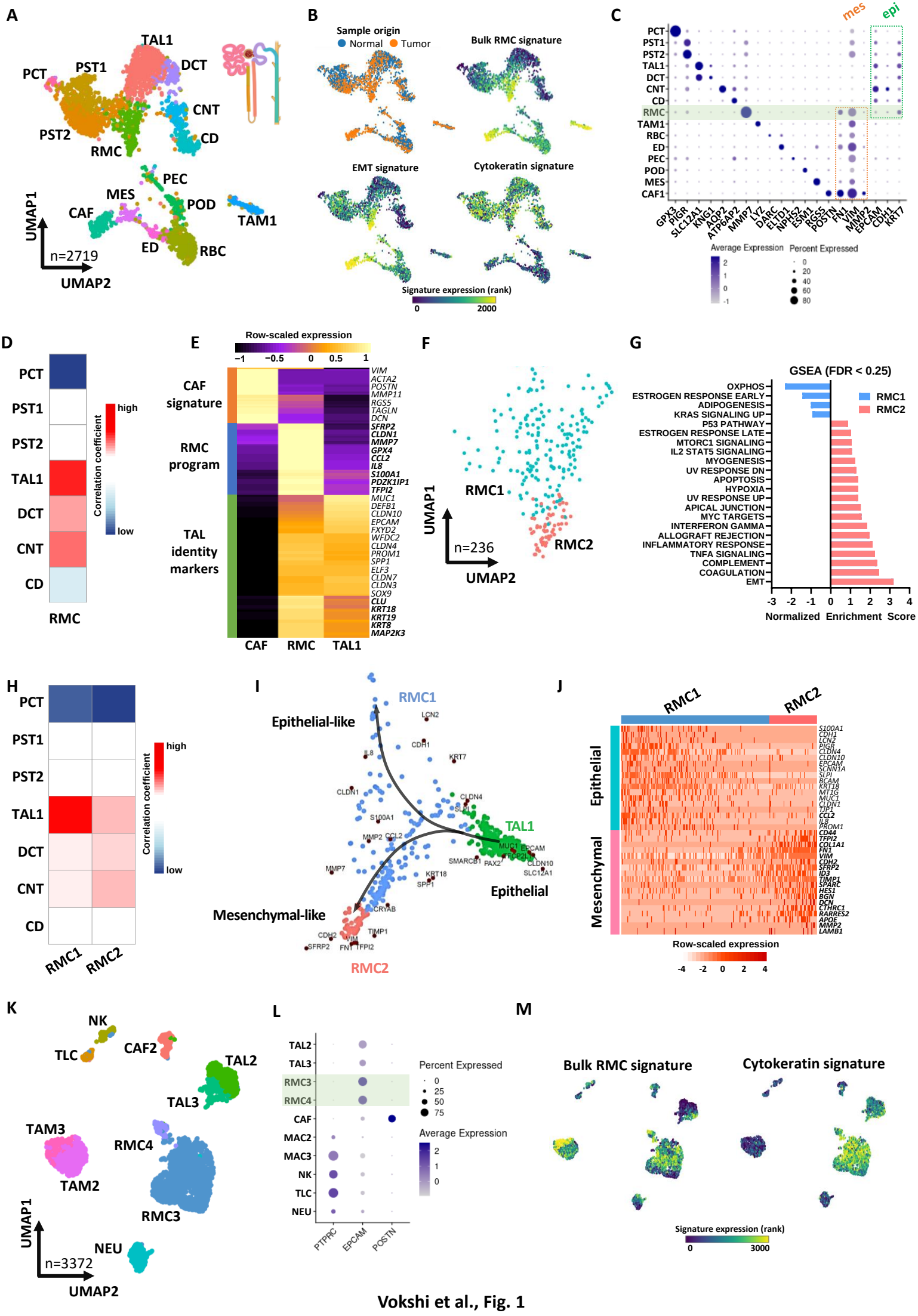

Vokshi et al., Fig. 1

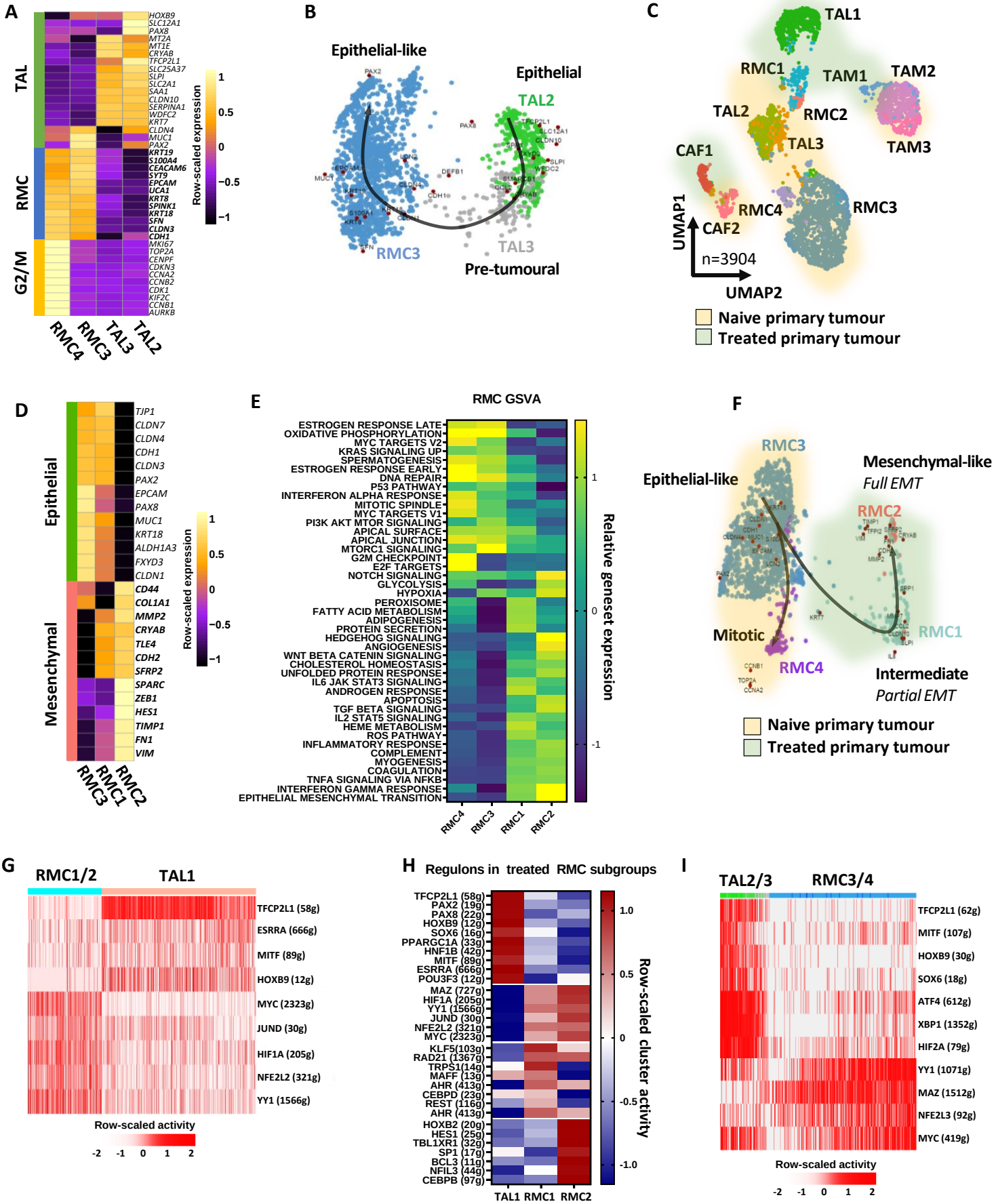

Vokshi et al., Fig. 2

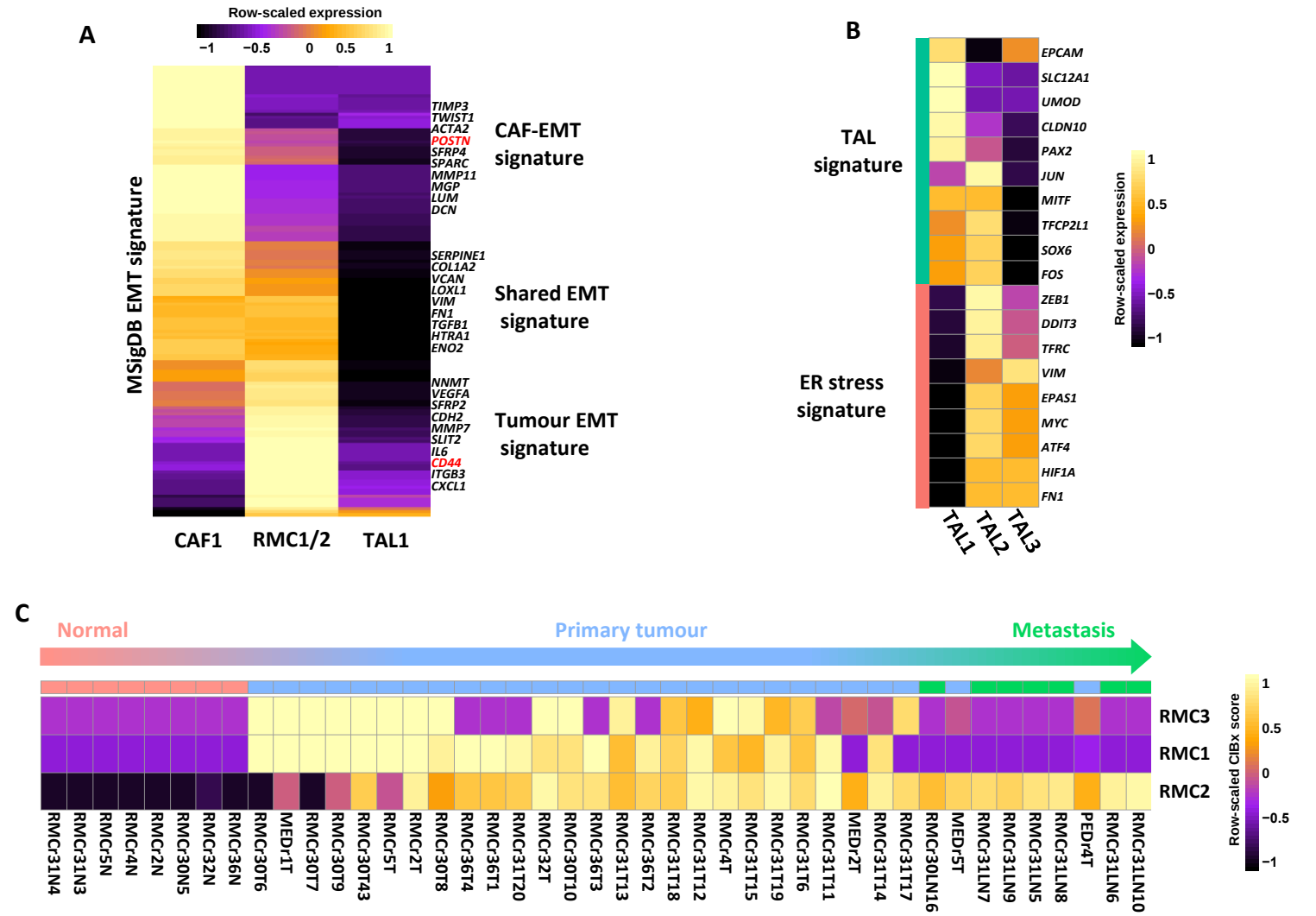

Vokshi et al., Suppl. Fig. 1

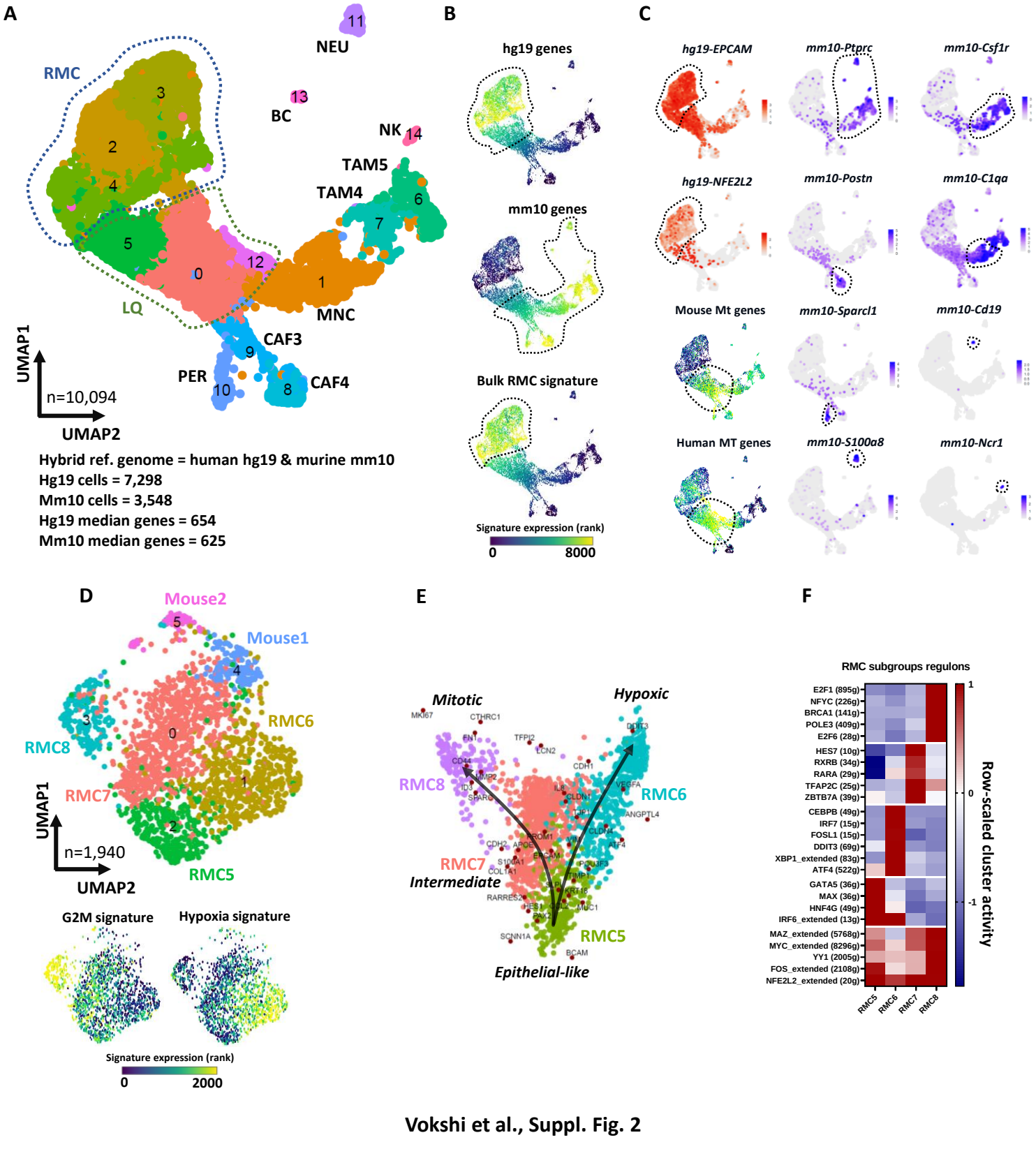

Vokshi et al., Suppl. Fig. 2

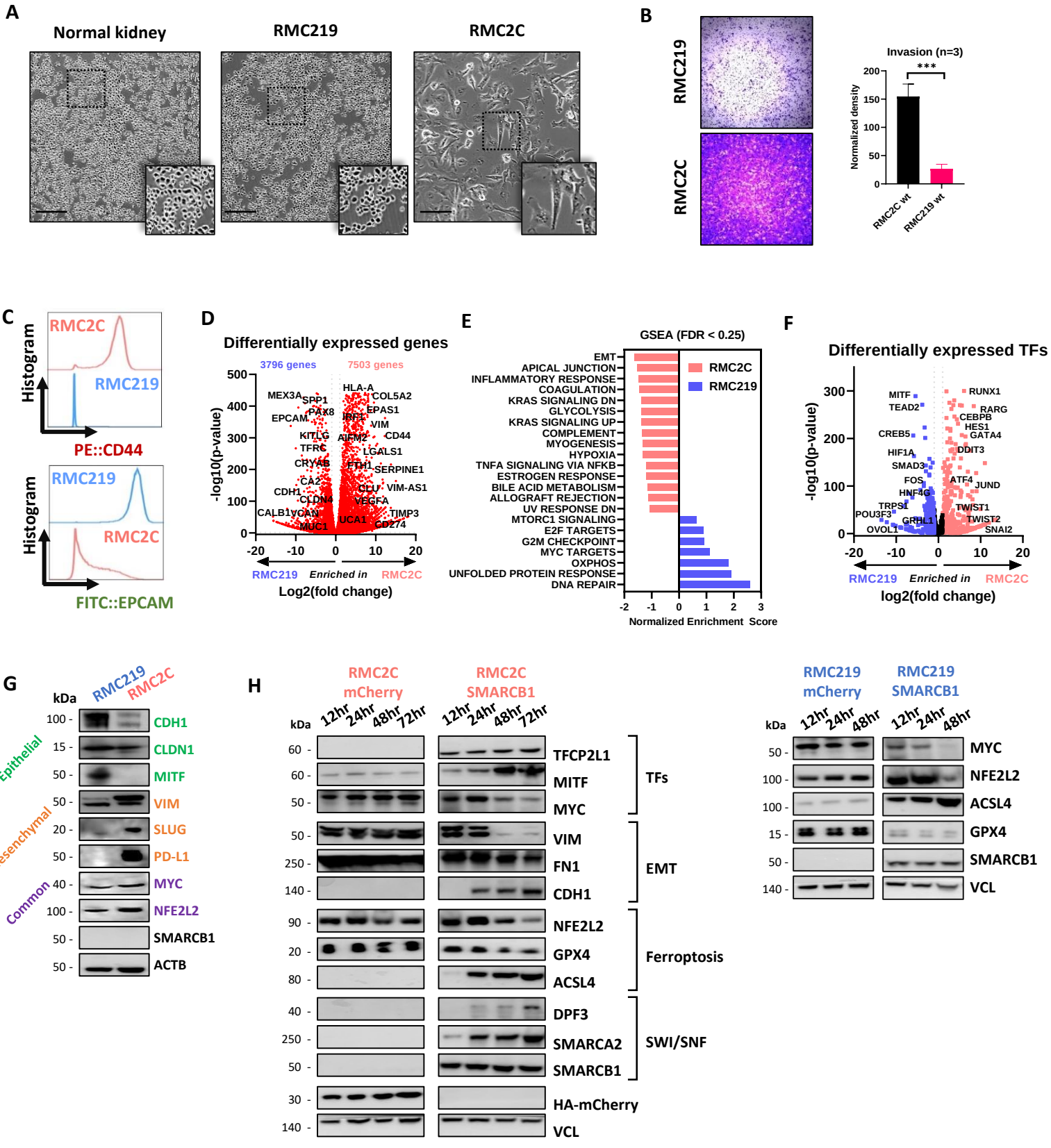

Vokshi et al., Fig. 3

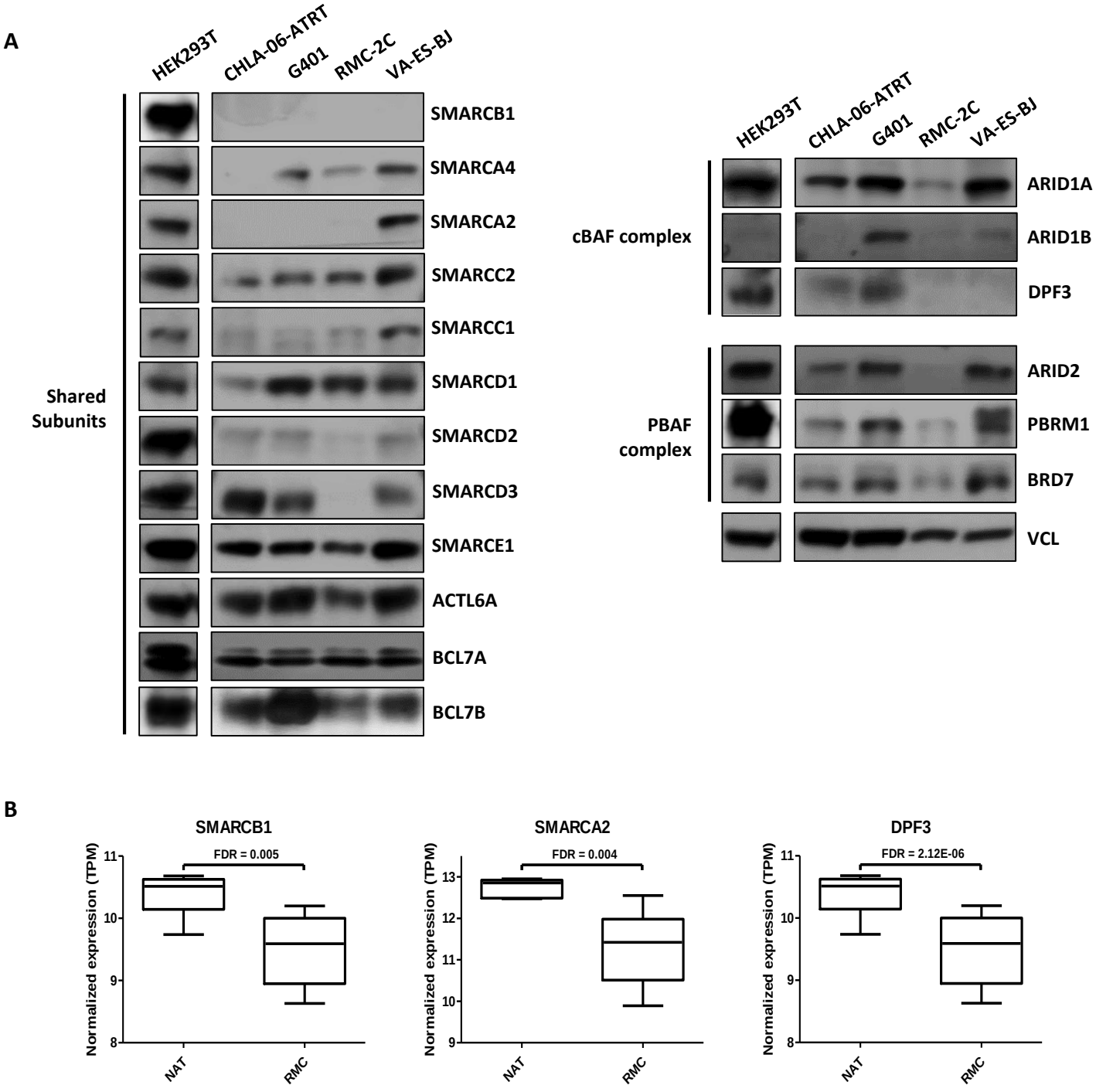

Vokshi et al., Suppl. Fig. 3

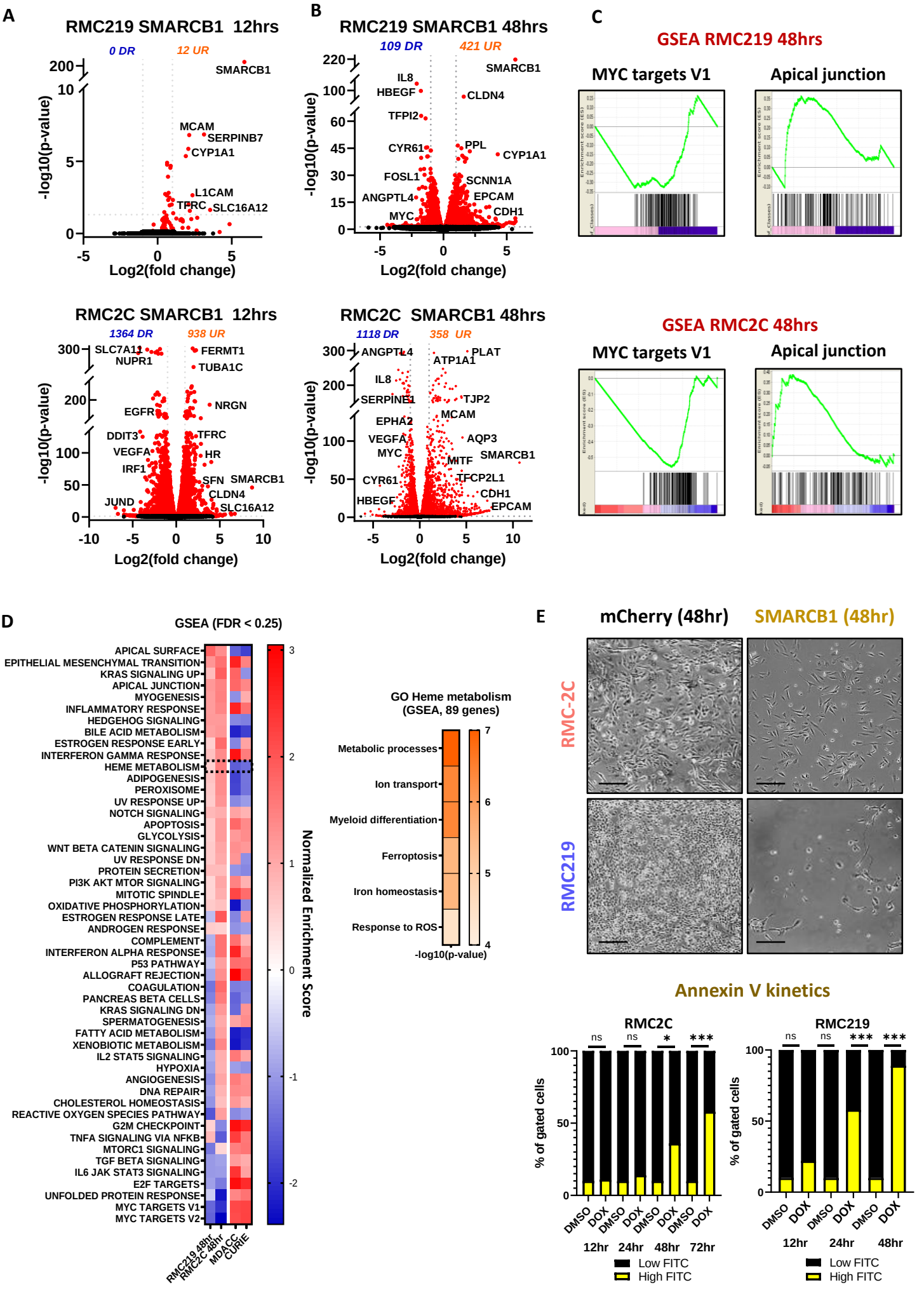

Vokshi et al., Fig. 4

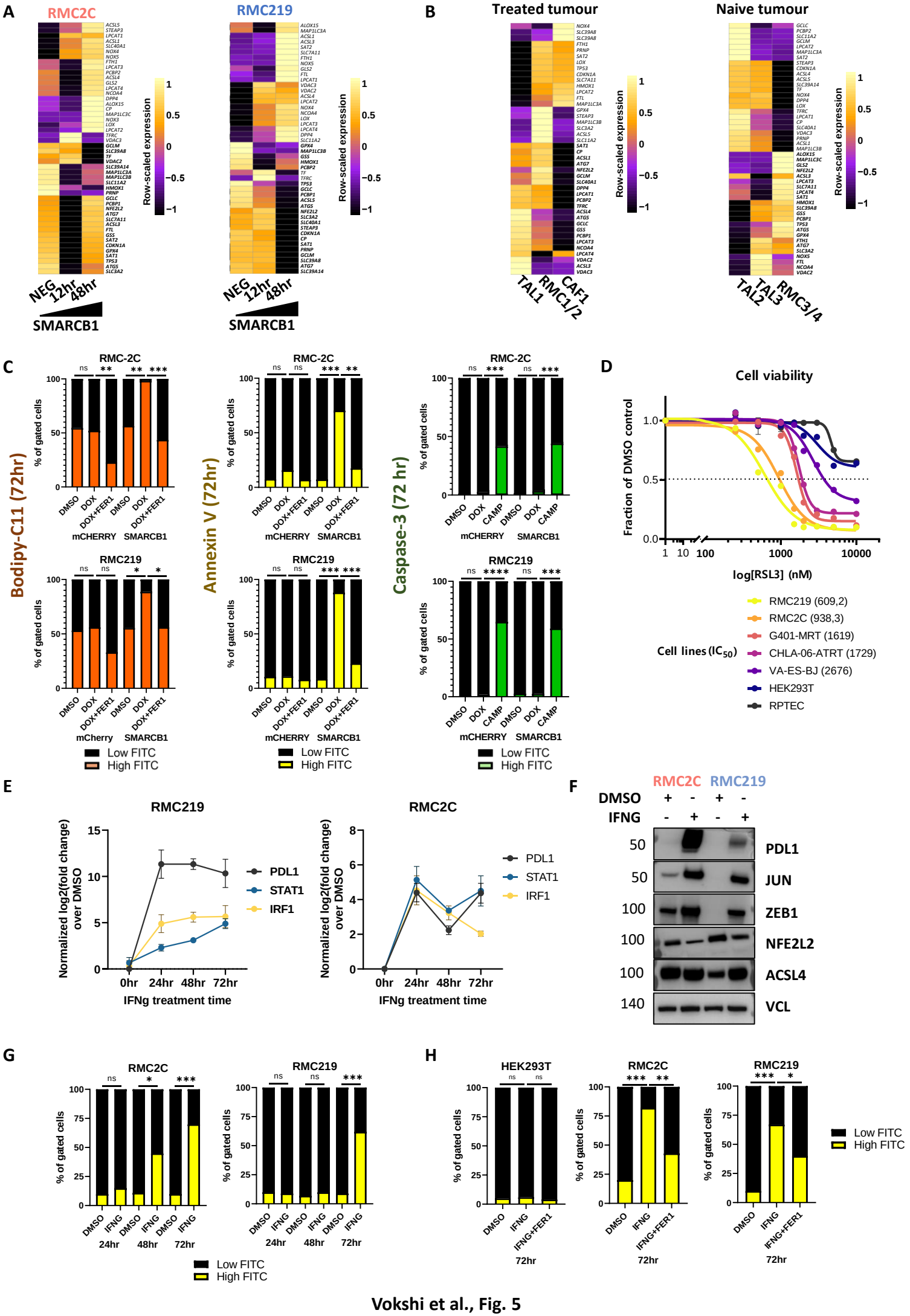

Vokshi et al., Fig. 5

A

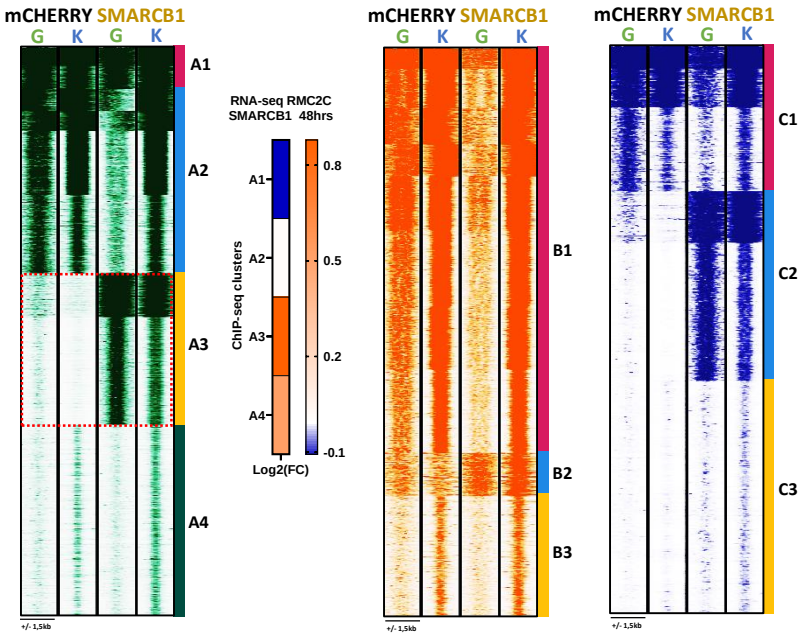

B

TOP MOTIFS FOUND IN CLUSTER A3

Consensus	Motif name	TF	E-value	# sites
	Grainyhead	TFCP2L1	2e-07	2381
	Homeobox	HOXB9	2.3e-06	1686
	E-box	MITF	4.5e-06	1639
	Paired box	PAX8	2.1e-05	1205
	HMG	SOX6	9.8e-09	734

C

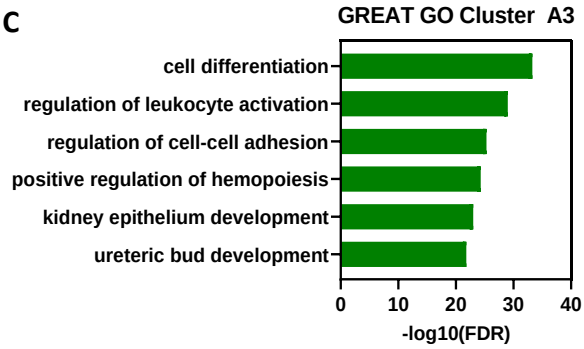

D

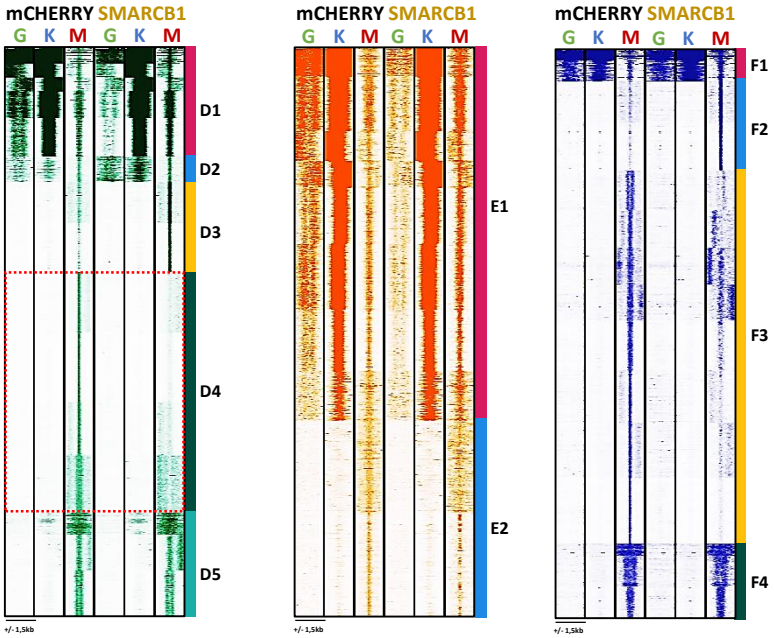

E

TOP MOTIFS FOUND IN MYC PEAKS (1000 BEST PEAKS RANKED BY SCORE)

Consensus	Motif name	TF	E-value	# sites
	E-box	MYC	1.9e-43	803
	Kruppel-related	KLF15	5.9e-37	386
	SMAD/NF-1	NFIA	5.6e-10	169
	PAS domain	HIF1A	6.5e-07	168
	Hairy-related	HES1	0.00052	116
	Jun-related	ATF3	7.1e-07	126

F

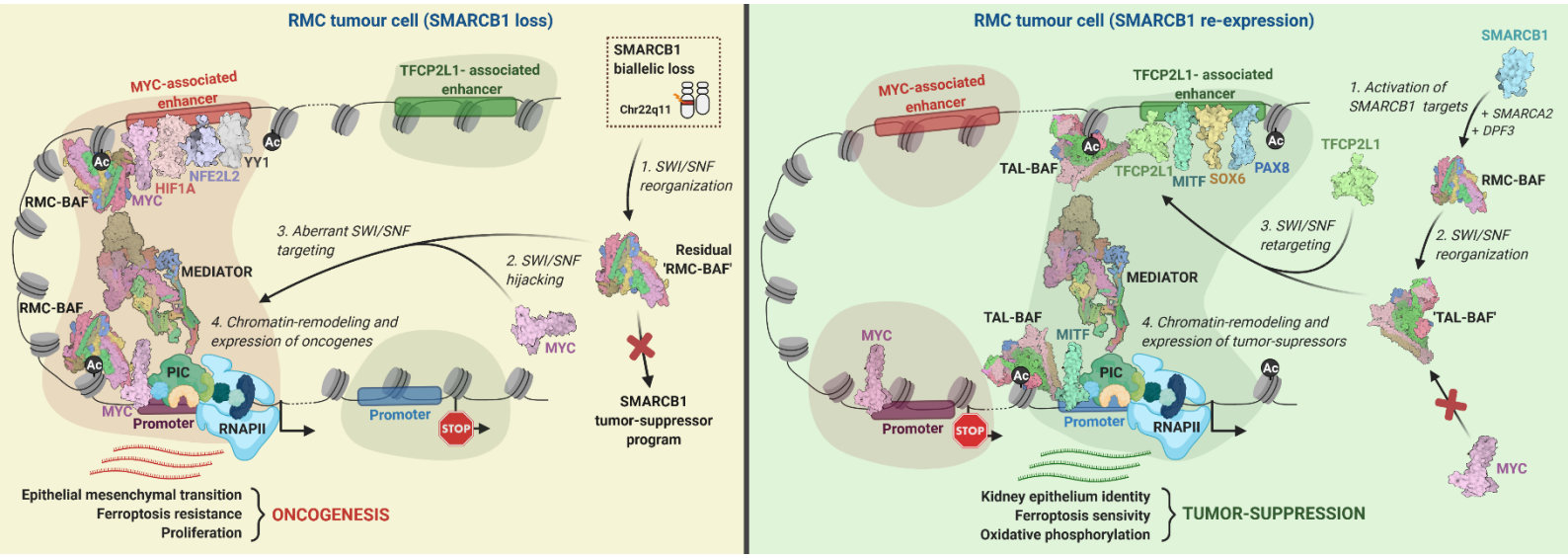

Vokshi et al., Fig. 6

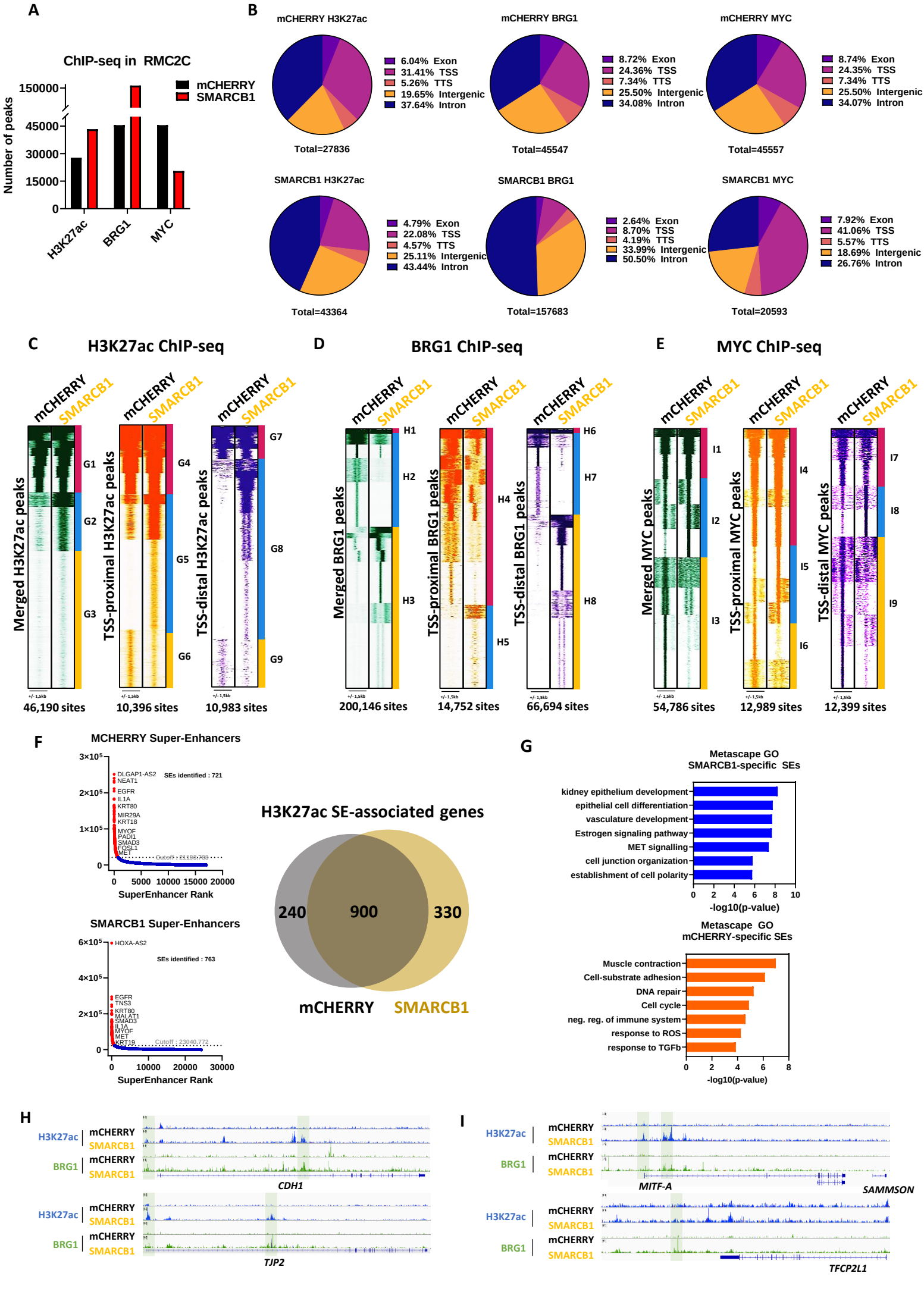

Vokshi et al., Suppl. Fig. 4

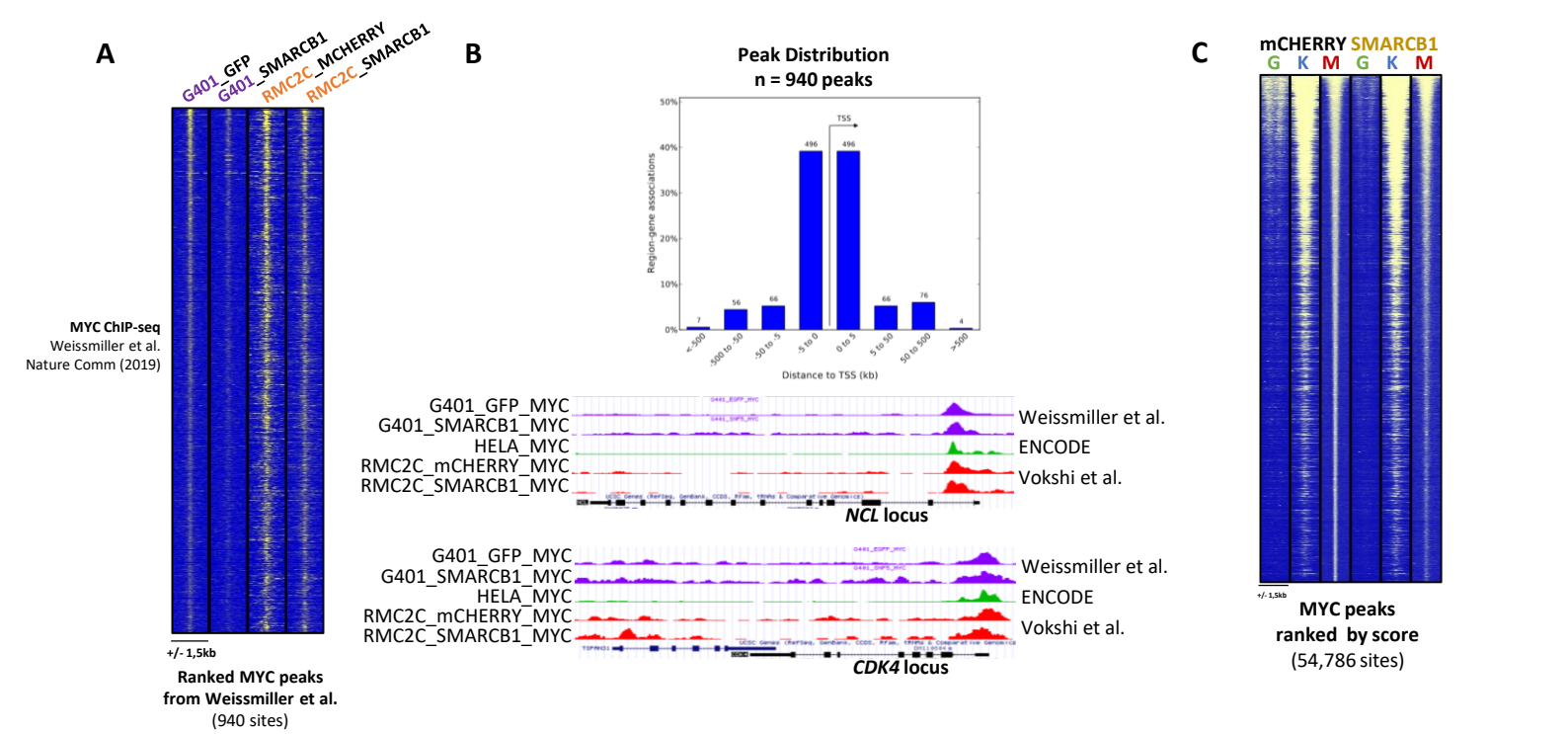

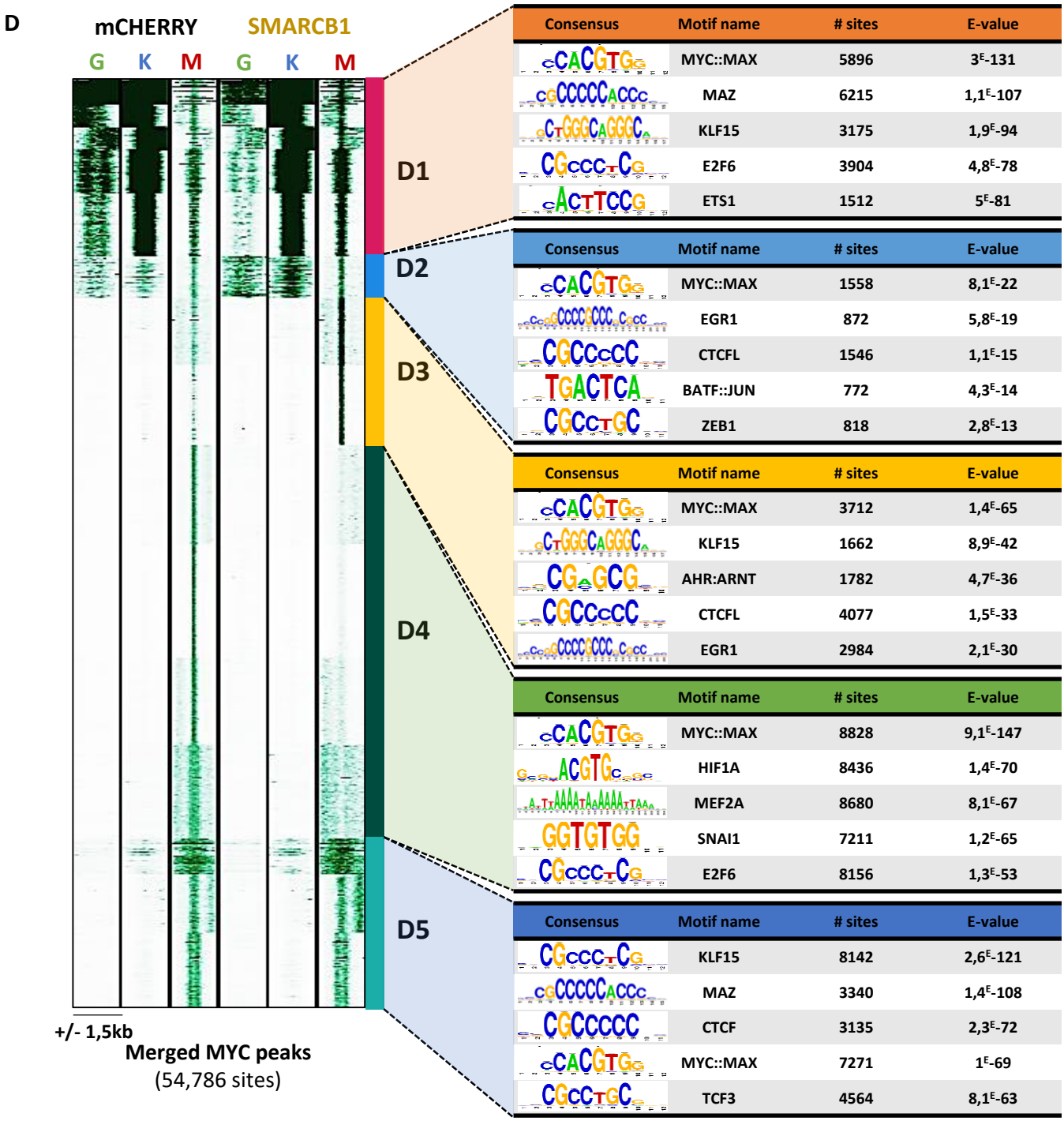

Consensus	Motif name	# sites	E-value
	MYC::MAX	5896	3^{E}-131
	MAZ	6215	$1,1^{E}$-107
	KLF15	3175	$1,9^{E}$-94
	E2F6	3904	$4,8^{E}$-78
	ETS1	1512	5^{E}-81

Consensus	Motif name	# sites	E-value
	MYC::MAX	1558	$8,1^{E}$-22
	EGR1	872	$5,8^{E}$-19
	CTCFL	1546	$1,1^{E}$-15
	BATF::JUN	772	$4,3^{E}$-14
	ZEB1	818	$2,8^{E}$-13

Consensus	Motif name	# sites	E-value
	MYC::MAX	3712	$1,4^{E}$-65
	KLF15	1662	$8,9^{E}$-42
	AHR:ARNT	1782	$4,7^{E}$-36
	CTCFL	4077	$1,5^{E}$-33
	EGR1	2984	$2,1^{E}$-30

Consensus	Motif name	# sites	E-value
	MYC::MAX	8828	$9,1^{E}$-147
	HIF1A	8436	$1,4^{E}$-70
	MEF2A	8680	$8,1^{E}$-67
	SNAI1	7211	$1,2^{E}$-65
	E2F6	8156	$1,3^{E}$-53

Consensus	Motif name	# sites	E-value
	KLF15	8142	$2,6^{E}$-121
	MAZ	3340	$1,4^{E}$-108
	CTCF	3135	$2,3^{E}$-72
	MYC::MAX	7271	1^{E}-69
	TCF3	4564	$8,1^{E}$-63

Vokshi et al., Suppl. Fig. 5

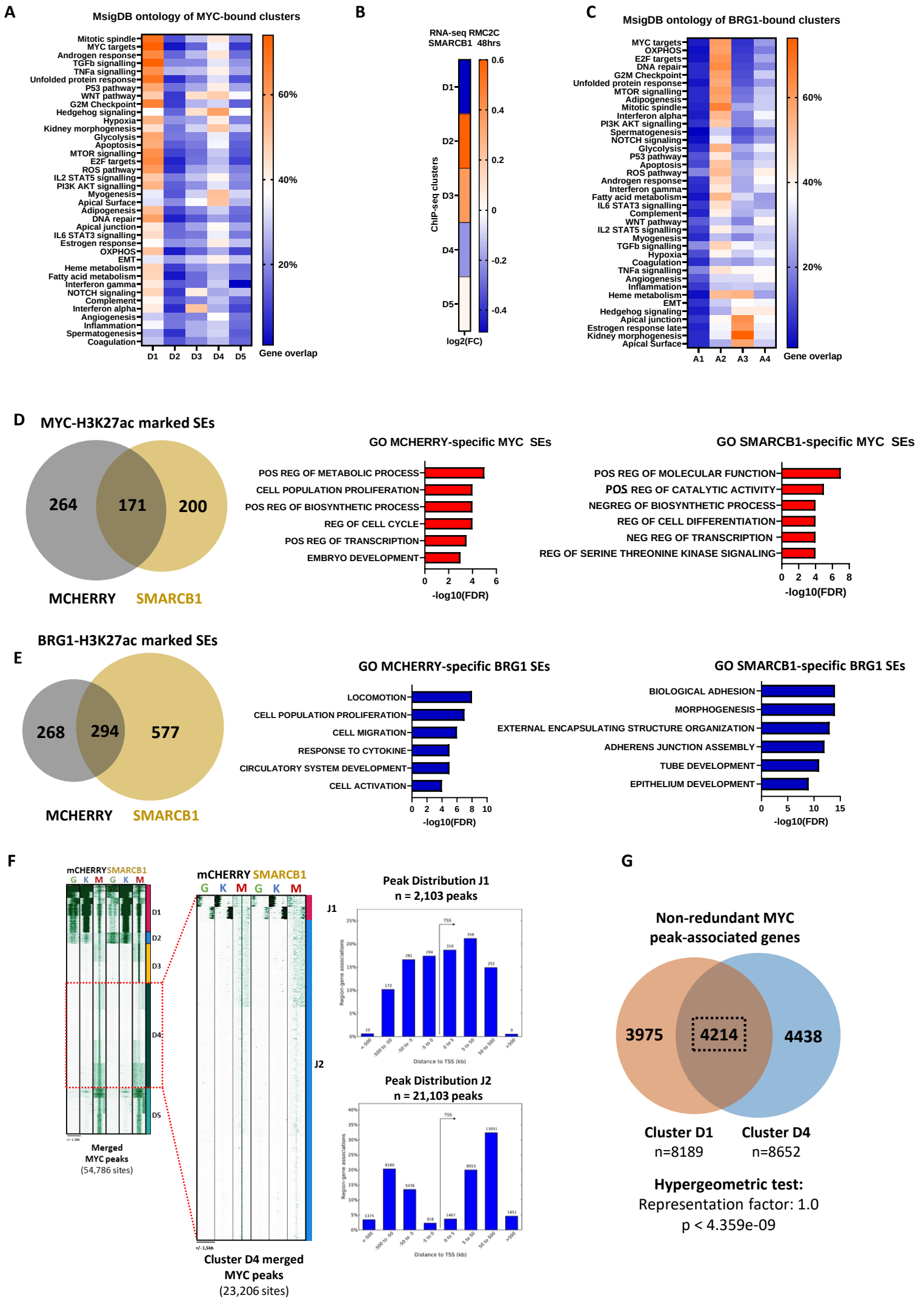

Vokshi et al., Suppl. Fig. 6